

Geostatistical Maps Of Malaria Patients And Their Correlation With Distribution Indicators In Southern Iran

Mehdi Shabanipoor¹, Maryam Kamali^{1*}, Abbasali Raz², Mohammad Saaid Dayer¹, Igor V. Sharakhov^{3,4}

Abstract

Malaria is a disease caused by the Plasmodium parasite, with a prevalent distribution among people in Africa and some Asian countries. Migration of people can play a significant role in the spread of malaria. This study aims to develop and investigate the geostatistical maps of malaria patients and their correlation with distribution indicators for disease management in the years 2016-2020 in southern Iran. Malaria patient data was obtained from the Ministry of Health and drawn as geostatistical maps. To achieve full understanding and alignment of the malaria patients' distribution patterns, five indices (Taylor, Iwao, Morisita, variance-to-mean ratio, and kappa) were used. The results showed that the aggregated distribution wave obtained from the geostatistical map in 2016, 2017, and 2018 were 2, 3, and 2, respectively. The Taylor index indicated a cumulative pattern due to higher sensitivity to the clustering of distribution in 2016 and 2017, with Taylor coefficients of 1.02 and 1.07, respectively. The Iwao coefficient showed random distribution of malaria patients. Furthermore, the alignment of maps with Morisita, variance-to-mean ratio, and kappa indices indicated that in 2016 and 2017, 15% and 20% of patients were cumulatively clustered, while 85% to 80% were randomly distributed in southern Iran. The distribution pattern of malaria patients in 2019 and 2020 was random according to all indices and geostatistical maps. In general, it can be concluded that the distribution of malaria patients in southern Iran does not show a critical phase. However, considering the migration of individuals from neighboring countries, passive and active surveillance should be carried out simultaneously to identify patients in subsequent years.

Keywords: cumulative, density, foci, distribution pattern.

Introduction

Malaria is a severe disease caused by Plasmodium parasites, transmitted to humans through the bite of infected female Anopheles mosquitoes. It is one of the leading causes of death worldwide. Malaria

¹ Department of Medical Entomology and Parasitology, Faculty of Medical Sciences, Tarbiat Modares University, Tehran, Iran.

² Malaria and Vector Research Group, Biotechnology Research Center, Pasteur Institute of Iran, Tehran, Iran

³ Department of Entomology, the Fralin Life Sciences Institute, Virginia Polytechnic Institute and State University, Blacksburg, VA, USA

⁴ Department of Genetics and Cell Biology and the Laboratory of Ecology, Genetics and Environmental Protection, Tomsk State University, Tomsk, Russia

is most prevalent in Africa and some Asian countries (Talapko, Škrlec, Alebić, Jukić, & Včev, 2019). According to the latest World Health Organization malaria report 2022, there were an estimated 247 million cases of malaria in 2021 in 84 malaria endemic countries, with estimated 593 000 cases of malaria deaths in 2021 (World Health Organization, 2022).

Migration of people can play a significant role in the spread of malaria. People moving from areas with high malaria transmission to areas with low transmission can introduce the disease to new regions. Conversely, individuals from low transmission areas who travel to high transmission areas may be at increased risk of contracting malaria. The spatial pattern of disease distribution involves studying the factors influencing the distribution of a particular disease in a specific region. This spatial distribution at a defined scale provides valuable insights into the disease. Understanding the spatial distribution of a disease using mathematical models can aid in ongoing planning for disease control in an area and help identify populations at risk after the presence of an infected individual with the potential to transmit the disease. To design effective malaria control strategies, it is essential to understand the spatio-temporal heterogeneity of malaria in a region (Gwitira et al., 2020). In a study conducted on geographic information systems and statistical distribution of passive malaria data in Zimbabwean health centers, the results indicated a significant positive spatial distribution in the study area, highlighting the heterogeneity of malaria in that region. By identifying sources and clusters with high disease rates using statistical models, regions with high-risk can receive more attention, and proper allocation of resources for malaria control in the area can be achieved (Gwitira et al., 2020).

Disease mapping is a visual representation of the geographical locations of patients, presenting general information about the occurrence of the disease within a population through spatial epidemiological data. Based on the results of these maps, planning and resource allocation needs can be monitored at all levels of healthcare, and appropriate interventions can be designed and tailored to areas that require further investigation, as well as communities that need more research to identify the disease cases (Samat & Mey, 2017). In a study conducted in Burundi, one of the countries in Sub-Saharan Africa, the results indicated that the northern regions of the country had a significantly higher risk of malaria compared to other areas. Based on the findings of this research, proposed GIS-based models for malaria risk mapping can significantly contribute to more informed decision-making and policy-making processes in planning for intervention and control of malaria risks. This, in turn, could lead to reducing the disease burden in the future and lowering vulnerability due to climate change (Hassaan, Abdrabo, & Masabarakiza, 2017). In a study conducted in Burkina Faso, West Africa, spatio-temporal analysis and prediction of malaria cases were performed using weather data and remote sensing. As a result of this study, an effective prediction model was developed using data obtained from detecting passive cases of the disease and using readily available and simple weather data. This analysis of malaria cases presents a powerful and forward-looking approach to identify and predict high-risk areas and periods of high disease transmission. It can also be utilized in the control and prevention of malaria (Bationo et al., 2021). In the effort to eliminate malaria, the National Malaria Control Program in Haiti, along with other international partners, implemented a campaign of interventions targeting high-risk communities exposed to malaria through evidence-based planning. A key component of this planning was the presentation of an up-to-date and endemic disease map along with seasonal characteristics of the country. This map was based on monthly case reports from 771 health centers across the country over a six-year period from 2014 to 2019. Additionally, a new modeling framework was introduced, using geostatistical modeling, to provide an estimation of the annual endemic pattern of malaria in Haiti (Cameron et al., 2021).

Developing a disease risk map is an effective and efficient tool for monitoring disease transmission and efforts towards disease control. In another study conducted in Ghana, Africa, geostatistical analysis and the probability map of malaria infection in children under 5 years old were devised using disease prevalence data. The results of this study indicated significant associations between malaria

prevalence and residential location (urban/rural), age, use of indoor residual spraying, socioeconomic status, and maternal education level (Ejigu, 2020).

In a study in Mozambique, East Africa, a spatial distribution map of malaria in children was created to design targeted and effective intervention methods for malaria control. The prevalence of malaria was found to be higher in rural areas, and the disease was increasing with the child's age while was decreasing with increasing household wealth index and maternal education level. Given the high prevalence of malaria in children in Mozambique, there is an urgent need for effective public health interventions. The risk maps generated in this study can be effectively used by malaria control program implementers to prioritize interventions in high-priority areas (Ejigu, 2020).

The aim of this research was to investigate the possibility of aligning mathematical models' distribution with geostatistical maps and determining the percentage of clustered distribution of patients. Geostatistical maps typically represent the level of infected patients in unclear and non-mathematical manner, but combining them with mathematical models, such as distribution indices, aids in better understanding and managing the disease. The main innovation of this article lies in the alignment of geostatistical maps with distribution indices. This type of modeling for disease distribution has been created for the first time in the world.

Methods

The study area for investigating the spatial distribution is located in the southern region of Iran, comprising the provinces of Fars, Kohgiluyeh and Boyer-Ahmad, Khuzestan, Bushehr, and Hormozgan (Figure 1). These provinces have a total area of approximately 295,607 square kilometers, constituting 18.2% of Iran's total land area. The total population of these provinces was recorded as 13,214,650 in the latest national census in 2016. These regions are connected to the Indian Ocean via the Oman Sea and the Persian Gulf. Factors such as humidity, vegetation cover, elevation, temperature, and water resources have an impact on the spread and distribution of malaria mosquitoes and the disease. These regions are susceptible to the expansion and dissemination of malaria due to these factors. To study the distribution of malaria in Iran, the data of malaria patients from 2016-2020, were first received from the Ministry of Health. The Ministry of Health workers had visited health centers and laboratories across the country during the 5 years (2016-2020) and confirmed the positive malaria cases. These data were organized in an Excel file, categorized by city and province. Next, the geographical coordinates (longitude and latitude) of all healthcare and medical centers in the country were inputted into the Surfer software to create a geostatistical map of malaria based on data anomalies. The analysis of this data was then conducted using the SPSS software to identify patterns and anomalies related to malaria distribution.

Three types of distribution patterns have been identified (Figure 2). These patterns help in understanding the precise forms of disease distribution.

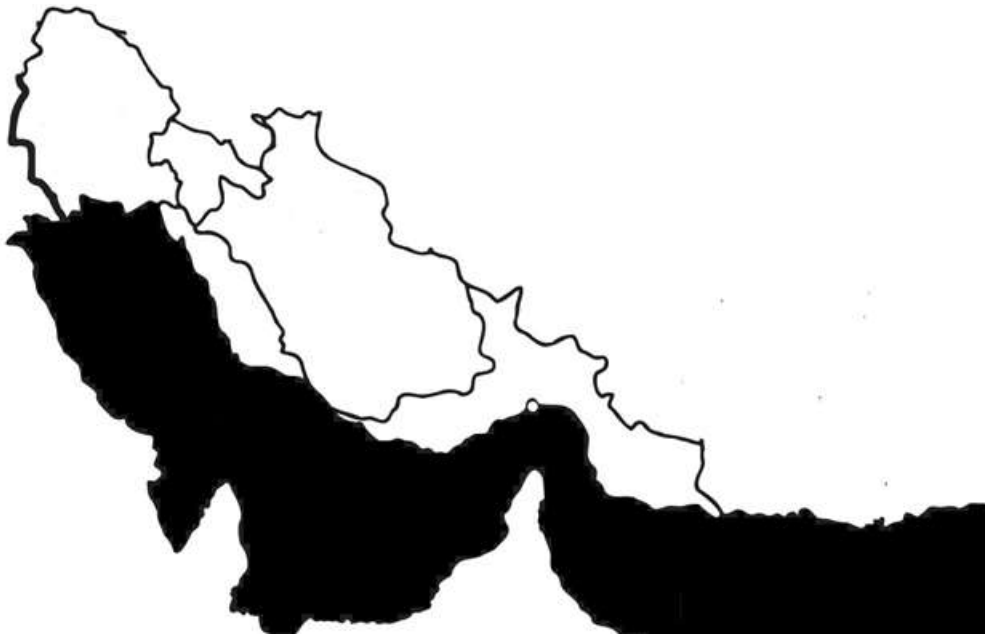


Figure 1. Geographical map of the studied area of southern Iran.

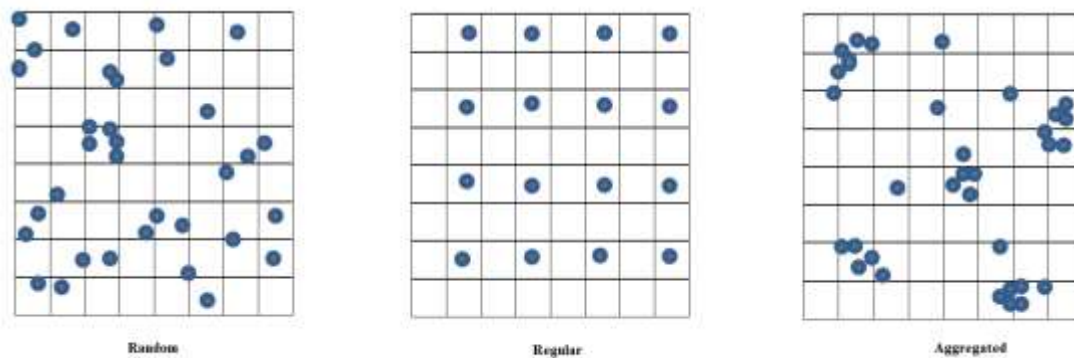


Figure 2. Three spatial point patterns: random, regularly dispersed, and clustered (aggregated or cumulative), distributions (Southwood, 1978).

In an aggregated distribution pattern, individuals within a population are grouped together in various locations within that population. This type of pattern often suggests that there are localized factors or specific conditions that lead to the clustering of individuals in certain areas.

In a regular distribution pattern, individuals are spaced at close and consistent intervals relative to others. This type of pattern implies that there is a uniform or systematic arrangement of individuals, often seen in situations where resources are evenly distributed or when there is competition for space.

In a random distribution pattern, individuals are scattered in a haphazard and irregular manner within a population. This type of pattern suggests that there is no specific order or organization to the arrangement of individuals, and their placement appears to be entirely random within the population. To measure and study the distribution of malaria, five indices were used: Taylor index (Taylor, 1984), Iwao's index (Southwood, 1978), K index (Southwood, 1978), variance-to-mean ratio (Poole, 1974), and Morisita index (Poole, 1974) (Table 1).

In the context of the Taylor relationship between population mean and variance, a regression equation (Table 1) was established, and the slope of this equation (b) was used as the Taylor index for

estimating population dispersion. This index is commonly employed as a statistical tool to illustrate the relationship between the population mean and variance, providing valuable insight into population distribution. Values smaller than, equal to, and greater than one b respectively indicate uniform, random and aggregated (clustered) dispersions.

In order to estimate the Iowa index between the mean (m) and the mean bulk index (m*), a regression relationship was established (Table 2), and its slope (β) was used as the Iowa index. Values smaller than, equal to, and greater than one β indicate uniform, random and aggregated dispersions, respectively.

To test the significance of the difference between the coefficients b (Taylor) and β (Iwao) with zero, the values of F and P were obtained from regression equations. To test the difference between the coefficients of Taylor and Iwao with one, equation t (equation 1) with degrees of freedom n-1 was used.

(1) $t = (\text{Slope} - 1) / SE_{\text{slope}}$

In this equation, Slope and SE_{slope} represent the coefficients of Taylor or Iwao and their standard errors in the regression equations (Tsai, Wang, & Liu, 2000).

Table 1: Estimator formula of distribution indexes.

Distributio n pattern	Specifications	Range			Relation
		Unifor m	Rando m	Cumul ative (aggre gated or cluster ed)	
Taylor index	mean (m) Variance (S ²)	b<1	b=1	b>1	$\text{Log} (S^2) = \text{Log} (a) + b \text{Log} (m)$
Iwao index)m *(Average mass index	β<1	β =1	β>1	$m^* = \alpha + \beta m$ $m^* = m + (\frac{S^2}{m} - 1)$
Variance to Mean ratio index	Variance to Mean index	ID <0	ID =0	ID >0	$\frac{S^2}{m}$ ID = $\frac{S^2}{m}$
Morisita index	Total number of individuals in all samples <i>n</i> N Total samples ni Number of people in sample number i	Iδ<1	Iδ =1	Iδ>1	$I\delta = N \frac{\sum n_i(n_i - 1)}{n(n - 1)}$
\hat{k} (Cumulativ e index	N Number of samples A_x The sum of the observed frequencies of	-	$\hat{k} < 8$	$\hat{k} > 8$	$N \text{Ln} \left(1 + \frac{m}{\hat{k}} \right) - \sum \left(\frac{A_x}{\hat{k}} \right) = 0$

	sampling units that have more than X				
--	--------------------------------------	--	--	--	--

The slope values of Taylor coefficient (b); The slope values of Iwao coefficient (β)

Results

The distribution pattern of the disease in southern Iran

Taylor’s Law: The statistics obtained from establishing a regression relationship between the logarithm of variance and the population mean (Taylor's law) in different quadrats are presented in Table 2 for investigating the distribution of malaria. The results of the regression analysis showed that in the years 2016 and 2017, the F value at the five percent significance level was consistently significant, and the coefficient of determination of the regression equations was relatively high. However, the F value was not significant for the years 2018, 2019, and 2020. The results indicate that the values of the Taylor's coefficient (b) for the years 2016 and 2017 were 1.02 and 1.07, respectively, as the calculated t-values were greater than the critical t-value. The null hypothesis of no difference between the b values and 1 is rejected, indicating a cumulative distribution of malaria in 2016 and 2017. Additionally, the values of the Taylor's coefficient (b) for the years 2018, 2019, and 2020 were 0.90, 0.82, and 0.78, respectively, and as the calculated t-values were less than the critical t-value, the null hypothesis of no difference between the b values and 1 is accepted, suggesting a random distribution of malaria in the years 2018, 2019, and 2020.

Table 2. Regression statistics for Taylor's method for five years of malaria cases in southern Iran

Year	$b \pm S_E$	R^2	F	T
2016	1.02±0.022	0.904	108.43*	3.79*
2017	1.07±0.012	0.938	152.19*	5.19*
2018	0.90±0.017	0.882	12.51	1.11
2019	0.822±0.025	0.824	8.2	0.91
2020	0.780±0.011	0.792	4.94	0.58

Iwao's method: The regression statistics obtained from the Iwao model are presented in Table 3. The results of the regression relationship between the mean population and the actual population showed that the values of β equal to 0.91, 0.98, 0.89, 0.79, and 0.71 correspond to the years 2016, 2017, 2018, 2019, and 2020, respectively. None of these coefficients showed a significant difference from 1, indicating that according to the Iwao's coefficient, the distribution of malaria patients in the southern region of Iran is random.

In comparison with the Taylor model, the Iwao model yielded more consistent regression coefficients with a higher R-squared value (R^2) and significantly lower standard errors of the regression coefficients. Therefore, it can be concluded that the Iwao index is more effective than the Taylor index in estimating the distribution coefficients of malaria patients in the five years studied in the southern region of Iran. Moreover, considering the data's variance being closer to the mean, the Iwao coefficient is a more appropriate indicator for estimating the distribution of malaria patients' population.

Table 3. Regression statistics for Iwao's method for five years of malaria cases in southern Iran.

year	$\pm S_E \beta$	R^2	F	T
2016	0.914±0.004	0.931	14.18	1.25
2017	0.984±0.004	0.944	15.75	1.49

2018	0.890±0.008	0.909	8.29	0.85
2019	0.799±0.011	0.878	4.11	0.68
2020	0.716±0.015	0.869	2.28	0.34

Based on the discrepancies between the Taylor and Iwao's coefficients in identifying the pattern of malaria cases distribution in the years 2016 and 2017, the percentage of agreement in the distribution of malaria cases for the five years of 2016-2020 is presented in Table 4. Over the five years, there was not a significant difference in the percentage of agreement with cumulative or random distributions. In the distribution of malaria patients, the percentage of agreement for the years 2016 to 2020 was lower with the cumulative distribution compared to the random distribution. These findings are consistent with the Iwao's index, indicating a random distribution of malaria patients during these years and confirm the error of the Taylor's index for the years 2016 and 2017. Additionally, the three indices, Morisita, Kappa, and variance-to-mean ratio, indicated that the distribution of malaria patients in southern Iran is random.

Table 4. Percentage of agreement in the frequency of malaria patients' distribution over the five years, 2016-2020, in southern Iran.

Dispersion indices						
	Variance-to-mean		Kappa		Morisita	
Year	Random	Cumulative	Random	Cumulative	Random	Cumulative
2016	83	17	85	15	87	13
2017	78	22	80	20	84	16
2018	95	5	91	9	100	0
2019	100	0	100	0	100	0
2020	100	0	100	0	100	0

Discussion

Analysis of malaria patients' dispersion maps

Maps of malaria patients' distribution in the year 2016-2020 in southern Iran are shown in Figures 3-7. Based on the distribution map, two clusters of cases are observed in the geographic latitudes 28, 29, and 30, and longitudes 51, 52, and 53 for the year 2016. Additionally, three clusters of cases are observed in the geographic latitudes 27, 28, 29, 30, and 30.5, and longitudes 50, 51, 52, and 53 for the years 2017 and 2018. These clusters represent areas with higher concentrations of malaria patients. In the years 2019 and 2020, the distribution of malaria patients is confirmed to be random, and no clustering is observed in Figures 4 and 5. Considering the Taylor coefficient (b), it can be concluded that the distribution of patients in the years 2018, 2019, and 2020 is consistent with the random pattern, as indicated by the spatial statistical maps. However, in the years 2016 and 2017, similar to the spatial maps, the pattern of distribution shows clustering, indicating the sensitivity of the Taylor coefficient to the clustering of malaria patients.

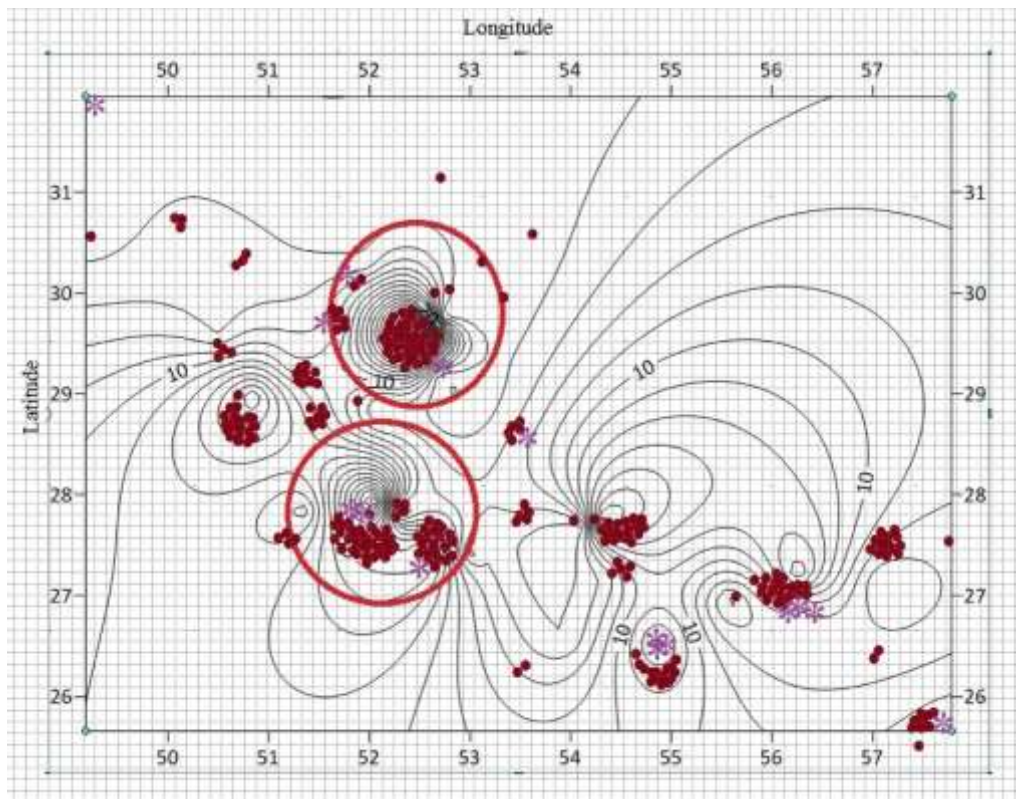


Figure 3. Distribution map of malaria patients in the south of Iran in 2016. (•) Foreign patients infected with malaria and (*) Iranian patients infected with malaria

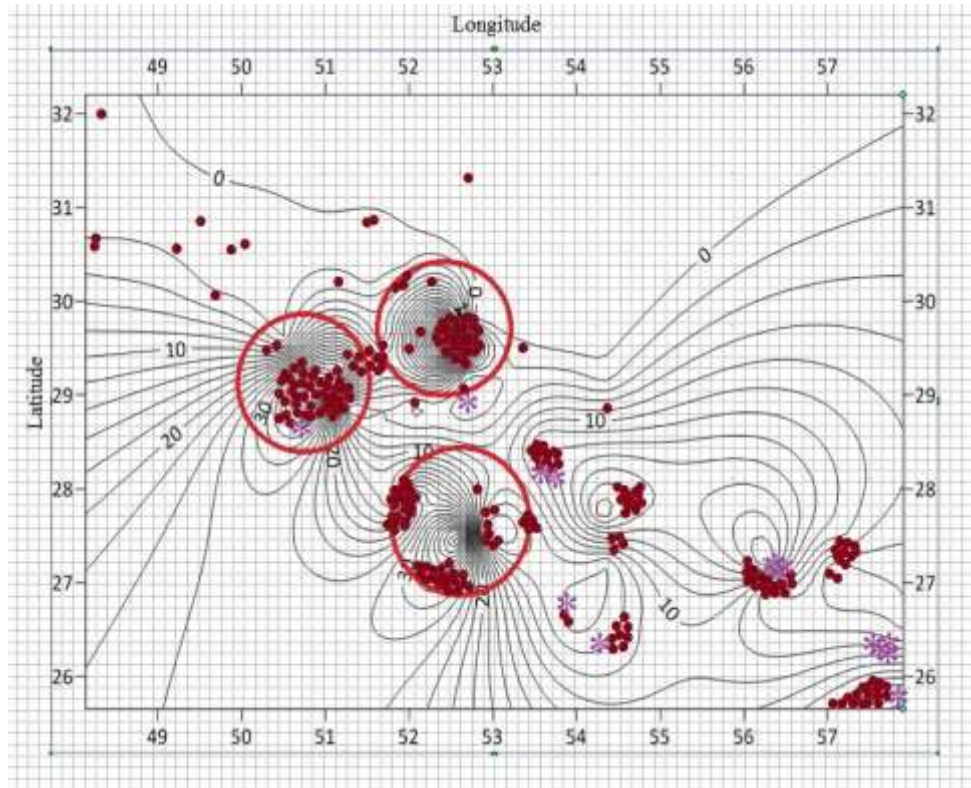


Figure 4. Distribution map of malaria patients in the south of Iran in 2017. (•) Foreign patients infected with malaria and (*) Iranian patients infected with malaria

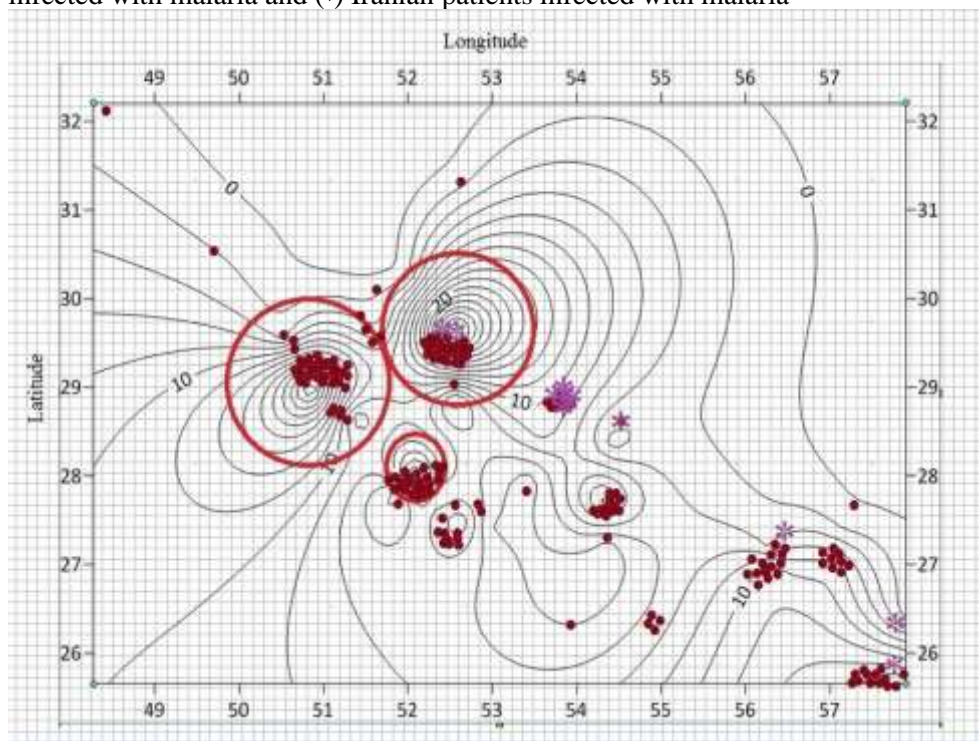


Figure 5. Distribution map of malaria patients in the south of Iran in 2018. (•) Foreign patients infected with malaria and (*) Iranian patients infected with malaria

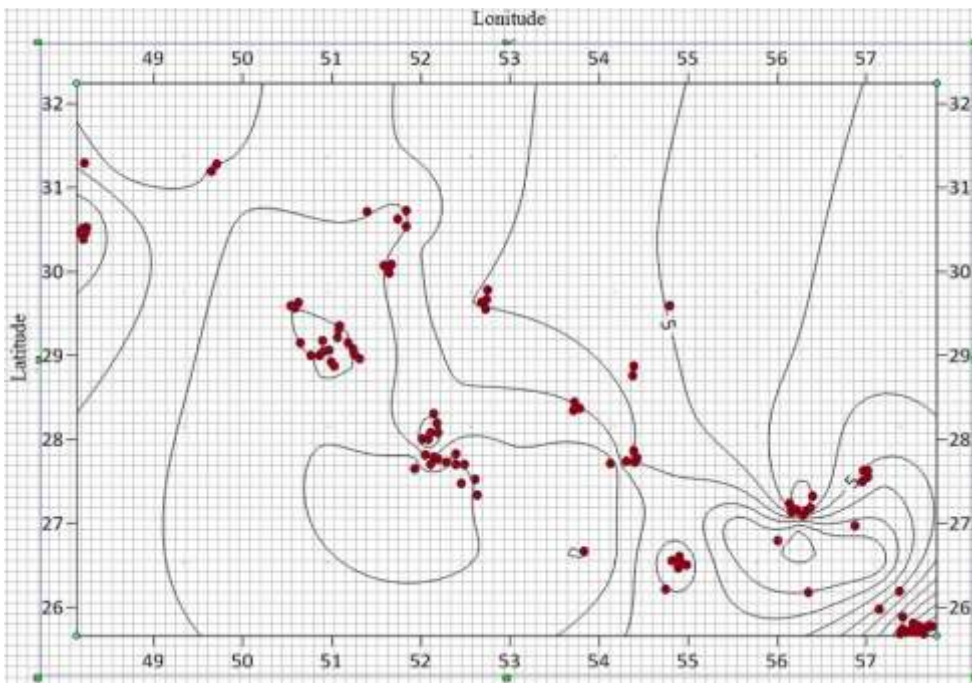


Figure 6. Distribution map of malaria patients in the south of Iran in 2019. (•) Foreign patients infected with malaria and (*) Iranian patients infected with malaria

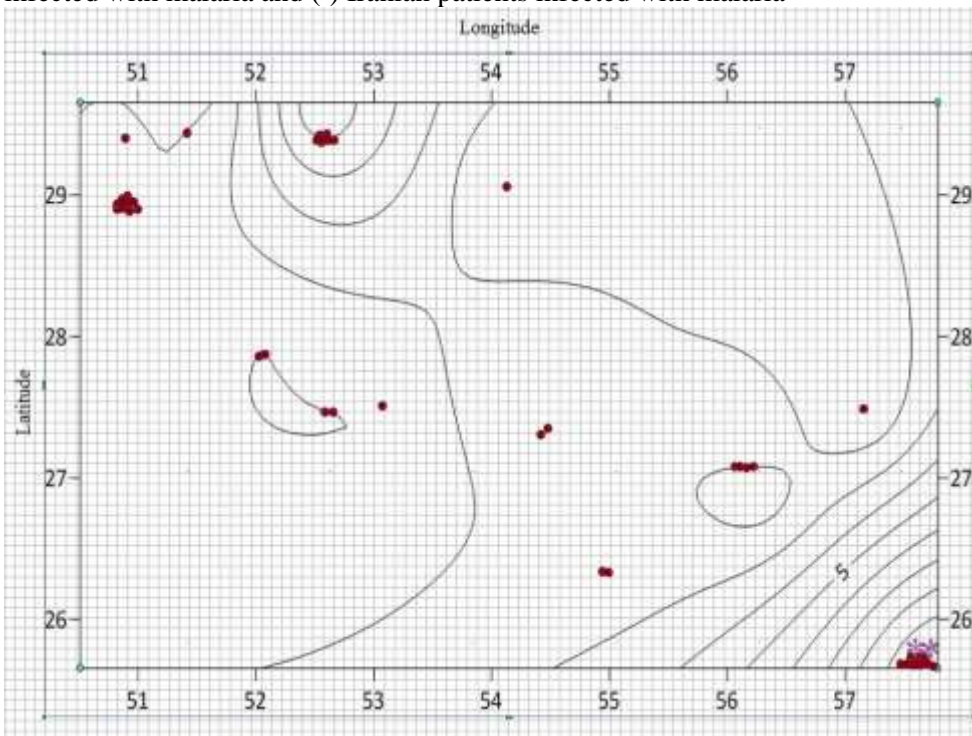


Figure 7. Distribution map of malaria patients in the south of Iran in 2020. (•) Foreign patients infected with malaria and (*) Iranian patients infected with malaria

The Iwao's index also suggests a random distribution of patients despite the two population means occurring in these latitudes. The percentages of agreement of the disease distribution with the

Morisita, the coefficient of variation, and the K index support the randomness and clustering of malaria distribution in accordance with the spatial patterns. The highest level of clustering for the disease is observed in the year 2017, with an average of around 20% on the map, which correlates to a great extent with the wave patterns on the map.

The highest percentage of random distribution is indeed observed in the years 2019 and 2020, which is 100% as shown in Figures 4 and 5. Most malaria cases in these maps are concentrated in the southeast of Iran, with fewer cases reported in the west and south. Moreover, the majority of malaria patients in Iran are immigrants from neighboring countries (Azizi et al., 2020). They settled collectively at the aforementioned latitudes of the regions in Iran. In 2016, 95% of the cases, in 2017, 95% of the cases, in 2018, 93% of the cases, in 2019, 91% of the cases, and in 2020, 100% of the cases were attributed to foreign nationals in these regions. It seems that one of the reasons for the cumulative distribution points in the map is that malaria case finding in Iran is more based on passive case detection (PCD) (Azizi et al., 2020). In passive case detection, detecting malaria cases is based on patients who usually have symptoms e.g.: fever, and seek care to health centers. As a result, it creates an accumulation point in a health and treatment centers. Passive case detection in all transmission settings is very critical for malaria surveillance, especially in elimination settings and disease-free areas to prevent re-establishment of malaria transmission (World Health Organization, 2018).

In passive surveillance, a health sector receives reports that are collected from hospitals, clinics, public health units, or other health centers. Passive case surveillance is a relatively inexpensive strategy to cover large areas, and provides critical information for community health monitoring. However, because passive surveillance depends on individuals in different institutions to provide data, it is difficult to control the quality and timeliness of the data (Nsubuga P, 2006). But the most important disadvantage of the passive case detection method is that not all cases of disease are reported, which can be problematic (Raeisi et al., 2013).

According to Figure 2, three dispersion patterns, random, clustered and uniform are depicted. Based on the results and the disease map obtained in 2016, Figure 3 of the disease map closely resembles a clustered dispersion pattern shown in Figure 2. Additionally, a significant portion of the map appears to be randomly scattered. Moreover, the dispersion type in Figure 4 is such that it closely resembles a clustered dispersion pattern.

The study of the density waves in the scattering pattern of the year 2016, as shown in Figure 3, indicates that the waves in regions with a geographical latitude of 28 to 32 and a geographical longitude of 54 to 58, have divergence and lack the ability to condense to create an aggregative state. In the geographical latitude of 31 to 32 and the geographical longitude of 49 to 58, there is a complete absence of any malaria cases in the form of continuous strip, which could possibly be due to the mountainous nature and lack of migratory population in this area.

The highest density wave, forming the aggregation pattern, is observed at the geographical latitude of 29.5 and 27.5, and the geographical longitude of 52 to 53. Cumulative foci of waves with lower density are indicated at the geographical latitudes of 26.5, 27, 27.5, and 28.5, and the geographical longitude of 50.5, 54.5, 55, 56 and 57. Generally, the results of the analysis of the density waves indicate that the geographical latitudes of 26, 28, and 30.5 are the entry points of the converging disease waves to create foci of aggregation.

The study of density waves in the distribution pattern in 2017, as shown in Figure 4, differs from 2016. The number of inputs for the formation of the cumulative distribution pattern is greater than in 2016. Convergent wave inputs from latitudes 26 to 32 have shown significant growth, indicating an influx of more patients from these areas. Convergent foci waves with high density are at the latitudes 29 to 30 and longitudes 50 and 50.5. Additionally, foci with low density are formed at latitudes 25, 26.5, 27, and 28 and at longitudes 52.5, 53, 54, 54.5, 56.5 and 57.

The analysis of wave formations creating the distribution pattern in 2018, as depicted in Figure 5, indicates a decreasing wave density pressure. Health networks in the southern regions of Iran, while monitoring the disease, have taken steps to control, surveillance, and treat malaria patients. Moreover,

the examination of the waves shows a reduction in the number of inputs leading to the formation of cumulative foci. The number of low-density foci has been decreasing rapidly compared to 2016 and 2017. Disease density waves for the formation of cumulative foci have shown less convergence, and the importance of health surveillance measures in reducing density waves is clearly evident, and successfully observed.

Furthermore, based on the dispersion models in Figure 2 and the correspondence with Figures 5, 6 and 7, the dispersion of individuals appears to be scattered and random. The distribution of individuals with irregular and non-clustered spacing is observed in all the mentioned figures. In Figure 5, the clustering density was low in some areas and bore a closer resemblance to random pattern.

According to Figure 6, the study of density waves in 2019 shows a significant difference compared to the years 2016 to 2018. Convergent wave inputs for the formation of cumulative foci have decreased drastically, and the number of high-density foci has significantly reduced. The dispersion pattern waves have rapidly diverged. The number of malaria patients has decreased, emphasizing the increased and more noticeable control and surveillance of the disease.

The examination of the wave formations creating the distribution pattern of malaria in 2020, as shown in Figure 7, indicates that the convergent waves for creating both large and small cumulative foci have decreased. Moreover, convergent waves for the creation of accumulation distribution patterns have transformed into divergent waves for random dispersion. The successful surveillance and control of malaria by the health networks showcased the Ministry of Health's efforts in 2020 to effectively prevent critical foci.

Conclusions

The analysis of malaria patients' dispersion maps alone can provide valuable insights into the clustering of malaria cases and help researchers and health authorities in disease control. However, combining these results with mathematical models and determining the percentage of clustering or randomness enables the development of precise management tools.

The findings obtained from this study can be utilized for various purposes, such as optimizing drug distribution, enhancing the control of disease vectors, and identifying potential outbreak hotspots in the future. It is recommended to continue monitoring the spatial distribution of the parasite in southern Iran and also track the improvement status of identified patients using geostatistical methods. These approaches can provide valuable information for better disease management and prevention strategies in the region.

Ethics approval and consent to participate

This project was reviewed and approved by the Research Ethic Committees of Tarbiat Modares University in Iran (Approval ID: IR.MODARES.REC.1402.097)

Consent for publication

All Authors read and approved the final manuscript.

Competing interests

The authors declare that they have no competing interests.

Funding

This project has received no funding.

References

Azizi, H., Davtalaab-Esmaili, E., Farahbakhsh, M., Zeinolabedini, M., Mirzaei, Y., & Mirzapour, M. (2020). Malaria situation in a clear area of Iran: an approach for the better understanding of the health service

- providers' readiness and challenges for malaria elimination in clear areas. *Malaria Journal*, 19. doi:10.1186/s12936-020-03188-7
- Bationo, C. S., Gaudart, J., Dieng, S., Cissoko, M., Taconet, P., Ouedraogo, B., . . . Moiroux, N. (2021). Spatio-temporal analysis and prediction of malaria cases using remote sensing meteorological data in Diébougou health district, Burkina Faso, 2016–2017. *Scientific Reports*, 11(1), 20027. doi:10.1038/s41598-021-99457-9
- Cameron, E., Young, A. J., Twohig, K. A., Pothin, E., Bhavnani, D., Dismar, A., . . . Battle, K. E. (2021). Mapping the endemicity and seasonality of clinical malaria for intervention targeting in Haiti using routine case data. *eLife*, 10, e62122. doi:10.7554/eLife.62122
- Ejigu, B. A. (2020). Geostatistical analysis and mapping of malaria risk in children of Mozambique. *PLOS ONE*, 15(11), e0241680. doi:10.1371/journal.pone.0241680
- Gwitira, I., Mukonoweshuro, M., Mapako, G., Shekede, M. D., Chirenda, J., & Mberikunashu, J. (2020). Spatial and spatio-temporal analysis of malaria cases in Zimbabwe. *Infectious Diseases of Poverty*, 9(1), 146. doi:10.1186/s40249-020-00764-6
- Hassaan, M., Abdrabo, M., & Masabarakiza, P. (2017). GIS-Based Model for Mapping Malaria Risk under Climate Change Case Study: Burundi. *Journal of Geoscience and Environment Protection*, 05, 102-117. doi:10.4236/gep.2017.511008
- Nsubuga P, W. M., Thacker SB, et al. (2006). *Health Surveillance: A Tool for Targeting and Monitoring Interventions*. Washington (DC): The International Bank for Reconstruction and Development / The World Bank.
- Poole, R. W. (1974). *An introduction to quantitative ecology* [by] Robert W. Poole. New York: McGraw-Hill.
- Raeisi, A., Gouya, M. M., Nadim, A., Ranjbar, M., Hasanzehi, A., Fallahnezhad, M., . . . Nikpour, F. (2013). Determination of Malaria Epidemiological Status in Iran's Malarious Areas as Baseline Information for Implementation of Malaria Elimination Program in Iran. *Iran J Public Health*, 42(3), 326-333.
- Samat, N. A., & Mey, L. W. (2017). Malaria Disease Mapping in Malaysia based on Besag-York-Mollie (BYM) Model. *Journal of Physics: Conference Series*, 890(1), 012167. doi:10.1088/1742-6596/890/1/012167
- Southwood, R. S. (1978). *Ecological methods : with particular reference to the study of insect populations / T.R.E. Southwood*. London : New York: Chapman and Hall ; Wiley.
- Talapko, J., Škrlec, I., Alebić, T., Jukić, M., & Včev, A. (2019). Malaria: The Past and the Present. *Microorganisms*, 7(6). doi:10.3390/microorganisms7060179
- Taylor, L. R. (1984). Assessing and Interpreting the Spatial Distributions of Insect Populations. *Annual Review of Entomology*, 29(1), 321-357. doi:10.1146/annurev.en.29.010184.001541
- Tsai, J., Wang, J.-J., & Liu, Y.-H. (2000). Sampling of *Diaphorina citri* (Homoptera: Psyllidae) on Orange Jessamine in Southern Florida. *The Florida Entomologist*, 83, 446. doi:10.2307/3496720
- World Health Organization. (2018). *Malaria surveillance, monitoring and evaluation: a reference manual*
- World Health Organization. (2022). *World malaria report 2022*. World Health Organization.